

# Blob Segmentation using Joint Space-Intensity Likelihood Ratio Test: Application to 3D Tumor Segmentation

Kazunori Okada, Umut Akdemir  
Siemens Corporate Research, Inc.  
Princeton, NJ, USA  
{kazunori, akdemir}@scr.siemens.com

Arun Krishnan  
Siemens Medical Solutions USA, Inc.  
Malvern, PA, USA  
arun.krishnan@siemens.com

## Abstract

*We propose a novel semi-automatic figure-ground segmentation solution for blob-like objects in multi-dimensional images. The blob-like structure constitutes various objects of interest that are hard to segment in many application domains, such as tumor lesions in 3D medical data. The proposed solution is motivated towards computer-aided diagnosis medical applications, justifying our semi-automatic and figure-ground approach. The efficient segmentation is realized by combining the robust anisotropic Gaussian model fitting and the likelihood ratio test (LRT)-based non-parametric segmentation in joint space-intensity domain. The robustly fitted Gaussian is exploited to estimate the foreground and background likelihoods for both spatial and intensity variables. We demonstrate that the LRT with the bootstrapped likelihoods is assured to be the optimal Bayesian classification while automatically determining the LRT threshold. A 3D implementation of the proposed algorithm is applied to the lung nodule segmentation in CT data and validated with 1310 cases. Our efficient solution segments a target nodule in less than 3 seconds in average.*

## 1. Introduction

The wide variety of object appearance characteristics and boundary geometry makes image segmentation a very difficult task. In past decades, a number of promising general-purpose approaches (e.g., classification/labeling/clustering [4, 1, 18, 11, 2] and curve-evolution [6, 20, 15]) have been proposed to solve this problem. In practice, however, structural assumptions of the target objects are often available beforehand thus can be exploited as a prior. The successful incorporation of such prior information plays a key role for realizing efficient and accurate segmentation solutions in general.

Our study focuses on developing an efficient segmentation solution for a class of blob-like structures captured in multi-dimensional images. We define the blob-like structures as roughly convex local intensity distributions whose

iso-level contours are approximately ellipsoidal with some irregularities that do not destroy the ellipsoidal topology. The intensity distribution itself may be multi-modal but it is assumed to be uni-modal under Gaussian blurring within an appropriate upper-bound of the smoothing bandwidth (i.e., Folklore Theorem [10]). Such class of data structures represents various objects of interest that are hard to segment in many application domains, such as CT lung tumor and PET hot spot segmentation in medical imaging applications [8] and mode analysis of multi-variate density estimation [2].

The presented work is motivated by the development of medical data segmentation solutions towards computer-aided diagnosis applications [17], where the overall system performance, including user-interaction factors, is concerned. In such context, semi-automatic solutions, requiring minimal user interactions, can be preferred to fully automated solutions for achieving better overall performance. For this reason, we choose a one-click figure-ground segmentation approach where a user provides a data point which roughly indicates a target/figure blob to be segmented out of arbitrary background. A successful solution to this problem depends on i) robustness against variation of the user-given initialization and the different scan settings in order to relieve the user's labor, ii) run-time efficiency, even with the high-dimensional data, in order to enhance the user-interactivity, and iii) high accuracy so that the user-interaction results in better performance than fully-automated solutions.

As a solution to the above depicted semi-automatic figure-ground segmentation, this paper presents a novel statistical segmentation framework which combines i) the robust anisotropic Gaussian fitting algorithm (solution A) and ii) a new non-parametric figure-ground segmentation algorithm using joint space-intensity likelihood ratio test (solution B). We have previously proposed the multi-scale joint segmentation and model fitting solutions for realizing the anisotropic Gaussian fitting by using the scale space mean shift [12] and the L-normalized scale space derivatives [14]. This provides robust and efficient characterization of the

target blob’s geometric structure, however such characterization remains as a parametric approximation of the true non-parametric boundary.

On the other hand, the likelihood ratio test (LRT) [3, pp.211-212] provides a basis for realizing an efficient non-parametric figure-ground segmentation. This approach offers the Bayesian optimal binary classification rule that is used to assign either fore- or back-ground label to each data point with a minimal Bayes error. It can describe irregular boundary accurately, given that likelihood functions for both fore- and back-ground are estimated accurately.

The main idea of the presented work is to model these likelihood functions used in the segmentation/classification solution B as functions of the anisotropic Gaussian fitted by the model fitting solution A. Due to the robustness of the solution A, we consequently achieve accurate likelihood estimation, resulting in robust and accurate non-parametric segmentation by the solution B. The likelihoods are modeled in the joint space-intensity domain for better accuracy. They are also estimated for each data instance, providing the robustness against different scan settings. The overall system is also efficient since both solutions are efficient.

One of the novelties of the presented work is to use the weighted likelihood model for the intensity likelihood estimation. This enables to model both foreground and background intensity likelihoods without explicitly assigned labels so that pre-segmentation and/or iteration is not required. This paper also contributes formal derivations, in the Bayesian framework, of the likelihood functions and *analysis support* which confines the sampling in the estimation processes. Such data support is a necessary concept for modeling the background probability distribution that is not naturally bounded. By parameterizing the support as a function of the fitted Gaussian, we show that the LRT with the formally derived likelihoods and analysis support is assured to be the optimal Bayesian classification while automatically determining the LRT threshold.

A number of previous studies are related to the proposed work. Leonaridis et al. [9] presented a range-data segmentation method based on iterative polynomial regression with model selection by winner-take-all. The combination of the model fitting and model selection used in their approach relates to the here proposed solution with the model fitting followed by the LRT classification. However, the proposed LRT classification approach offers a more theoretically sound segmentation/model selection principle. We have previously proposed a joint-domain mean shift-based segmentation method which exploits the prior model fitting process [13]. The runtime efficiency of this solution is, however, reduced when the size of tumors to be analyzed increases. The proposed method is more efficient than these methods by avoiding expensive iterations. In their region competition framework, Zhu and Yuille [20] demonstrated

that the motion equation of boundary points can be expressed as a function of a likelihood ratio test between two adjacent regions. Since the proposed segmentation framework follows the label classification approach, rather than the curve evolution approach, the similarity is not directly exploitable. Pastor et al. [16] presented a diesel spray image segmentation method using a likelihood ratio test. Although their LRT-based segmentation is motivated similarly to ours, our method offers a more sophisticated likelihood modeling.

This paper is organized as follows. Section 2 and 3 introduce the two-step segmentation solution with the robust anisotropic Gaussian model fitting and the joint likelihood ratio test, respectively. Section 4 describes our likelihood modeling solutions. The likelihood models and corresponding analysis support are formally derived in this section. A 3D implementation of the solution is evaluated by using a set of high resolution chest CT scan data. Section 6 describes the results of our experiments, followed by discussions in Section 7.

## 2. Robust Anisotropic Gaussian Intensity Model Fitting

The proposed semi-automatic (one-click) blob segmentation algorithm consists of two steps. The first step is a pre-processing with robust anisotropic Gaussian fitting. Readers are referred to [12, 14] for the details of this procedure. The following briefly summarizes its main ideas. Given an initial marker  $\mathbf{x}_p$  indicating a rough location of the target structure (e.g., tumor), the procedure provides the estimated target center  $\mathbf{u}$  and the anisotropic spread  $\Sigma$  in the form of Gaussian function:  $\Phi(\mathbf{x}; \mathbf{u}, \Sigma) = |2\pi\Sigma|^{-1/2} \exp(-1/2(\mathbf{x} - \mathbf{u})^t \Sigma^{-1}(\mathbf{x} - \mathbf{u}))$ . The volume of interest (VOI)  $\Omega$  is defined as the extent of our data analysis given by a fixed-size  $N$ -D window centered at  $\mathbf{x}_p$ . The data to be analyzed is expressed by  $I(\mathbf{x}) \in \mathcal{R}^+$  where  $\mathbf{x} \in \Omega \subset \mathcal{R}^N$  is  $N$ -D coordinate indicating data (pixel/voxel) location. The multi-scale joint model fitting and segmentation is realized by evaluating Gaussian scale space of  $I(\mathbf{x})$  [19, 7]:  $L(\mathbf{x}; h_i) = I(\mathbf{x}) * \Phi(\mathbf{x}; \mathbf{0}, h_i \mathbf{I})$ . For a set of discrete analysis scales  $\{h_i\}$ , the center  $\mathbf{u}_i$  and the spread  $\Sigma_i$  are estimated, resulting in a set of estimate pairs  $\{(\mathbf{u}_i, \Sigma_i)\}$ . The stability-based scale/bandwidth selection using the Jensen-Shannon divergence [12] selects the most stable estimate  $(\mathbf{u}^*, \Sigma^*)$  among this set. At each analysis scale  $h_i$ , the mean  $\mathbf{u}_i$  is estimated by the convergence of the majority of data points sampled around  $\mathbf{x}_p$  by using the scale space mean shift [12]:

$$\mathbf{m}(\mathbf{x}, h_i) = \frac{\int \mathbf{x}' \Phi(\mathbf{x} - \mathbf{x}'; h_i) I(\mathbf{x}') d\mathbf{x}'}{\int \Phi(\mathbf{x} - \mathbf{x}'; h_i) I(\mathbf{x}') d\mathbf{x}'} - \mathbf{x} = h_i \frac{\nabla L(\mathbf{x}; h_i)}{L(\mathbf{x}; h_i)}.$$

The anisotropic spread  $\Sigma_i$  is estimated by symmetric-positive-definite-constrained least-squares solution of a set of linear matrix equations consisting of  $L$ -normalized scale

space derivatives [14]. Such derivatives are sampled along the convergent trajectories of the scale space mean shift initialized at points sampled around the estimated center  $\mathbf{u}_i$ .

The resulting multi-scale Gaussian model fitting solution is robust against i) the influence from non-target neighboring structures by using the robust estimation technique to remove outliers according to the mean shift convergence, ii) the non-Gaussianity or misfit of the data by using the stability-based scale selection criterion that is insensitive to such modeling errors, and iii) the varying initialization  $\mathbf{x}_p$  by using the robust extension of least-squares approach. The solution is also efficient because it is based on a local sampling, guided by the mean shift procedure, which avoids the expensive construction of the scale space over the full data space.

### 3. Figure-Ground Segmentation by Likelihood Ratio Test

This section introduces the second step of our segmentation solution. At each data point  $\mathbf{x} \in \Omega$ , we are given its corresponding intensity value  $\alpha = I(\mathbf{x})$ . Treating both  $\mathbf{x}$  and  $\alpha$  as independent random variables, we assume that joint likelihood functions of  $(\mathbf{x}, \alpha)$  can be estimated for the foreground (inside or part of a target tumor)  $f(\mathbf{x}, \alpha|in)$  and for the background (outside of the tumor)  $f(\mathbf{x}, \alpha|out)$ . The space-intensity joint likelihoods can be factorized for the foreground as  $f(\mathbf{x}, \alpha|in) = f(\mathbf{x}|in)f(\alpha|\mathbf{x}, in)$  and for the background by replacing *in* by *out*. In order to bootstrap the likelihood efficiently from a single data instance, we approximate the conditional intensity likelihood  $f(\alpha|\mathbf{x})$  by  $f(\alpha)$ , assuming the independence,

$$f(\mathbf{x}, \alpha|in) = f(\mathbf{x}|in)f(\alpha|in) \quad (1)$$

$$f(\mathbf{x}, \alpha|out) = f(\mathbf{x}|out)f(\alpha|out) \quad (2)$$

where  $f(\mathbf{x}|in)$  and  $f(\alpha|in)$  ( $f(\mathbf{x}|out)$  and  $f(\alpha|out)$ ) denote marginal foreground (background) spatial and intensity likelihood functions, respectively. The two variables are not independent in general, however our experimental results shown later indicate that their dependence seems to be weak, resulting in good segmentation results. The space-intensity joint likelihood ratio  $r(\mathbf{x})$  is then defined by,

$$r(\mathbf{x}) \equiv \frac{f(\mathbf{x}, \alpha|in)}{f(\mathbf{x}, \alpha|out)} = \frac{f(\mathbf{x}|in)f(\alpha|in)}{f(\mathbf{x}|out)f(\alpha|out)} \quad (3)$$

A generic figure-ground segmentation solution is realized by determining the foreground-background membership of (or binary classification of) each voxel data point within the VOI by performing the likelihood ratio test,

$$\mathbf{x} \in \Omega \longleftarrow \begin{cases} in & \text{if } r(\mathbf{x}) \geq th \\ out & \text{otherwise} \end{cases} \quad (4)$$

where  $th$  is a threshold which depends on the normalization factors of the foreground and background likelihoods. The solution provides the minimal-error Bayesian classification given an appropriate threshold value [3]. In the following sections, we will show that modeling the likelihoods within a specific support region assures the Bayesian optimality at  $th = 1$ . Therefore,  $th = 1$  will be used throughout this paper. The overall framework provides a generic and efficient segmentation principle which i) combines the geometric and intensity information probabilistically and ii) reduces the segmentation ambiguity at boundary region by comparing explicit statistical models of foreground and background statistics.

## 4. Modeling Likelihood Functions

In order to realize the segmentation outlined above in Eq.(4), we must model four likelihood functions for spatial and intensity factors and for inside and outside the target structure:  $f(\mathbf{x}|in)$ ,  $f(\mathbf{x}|out)$ ,  $f(\alpha|in)$ , and  $f(\alpha|out)$ . The main idea exploited here is to derive these likelihoods as functions of the outcome of the robust Gaussian model fitting for efficient and accurate likelihood estimation. Instead of modeling these functions for a class of all possible blobs (e.g., tumors), they are independently estimated for each data instance.

### 4.1. Spatial Likelihood Functions

This section formally derives the definition of the foreground and background spatial likelihoods in the Bayesian framework. We assume the  $N$ -D Gaussian function  $\Phi(\mathbf{x}; \mathbf{u}, \Sigma)$ , fitted by the procedure described in Section 2, approximates a probability distribution of location  $\mathbf{x}$  being the blob center or mean  $\mathbf{u}$ . Suppose that this probability distribution can be interpreted as the conditional probability distribution  $P(\mathbf{x}|in)$  of  $\mathbf{x}$  being part of the target blob structure,

$$P(\mathbf{x}|in) \equiv \Phi(\mathbf{x}; \mathbf{u}, \Sigma) \quad (5)$$

This holds true if surface geometry of the target structure is approximately convex, which assures the mean is located inside of the structure. In many applications, such as the tumor segmentation, this is a reasonable assumption.

The conditional probability distribution for the background  $P(\mathbf{x}|out)$  is ill-defined because the background extends to an infinite range of the data space  $\mathbf{x}$ . In order to define such a pdf, a window that confines observations of the random variable  $\mathbf{x}$  has to be introduced so that a normalization becomes possible. We call such a data space window *analysis support* denoted by  $S \subset \Omega$ . The modeling of such support will be discussed later in Section 4.3.

We define a pair of conditional probability distribution functions over the support,  $\bar{P}(\mathbf{x}|in)$  and  $\bar{P}(\mathbf{x}|out)$ , which

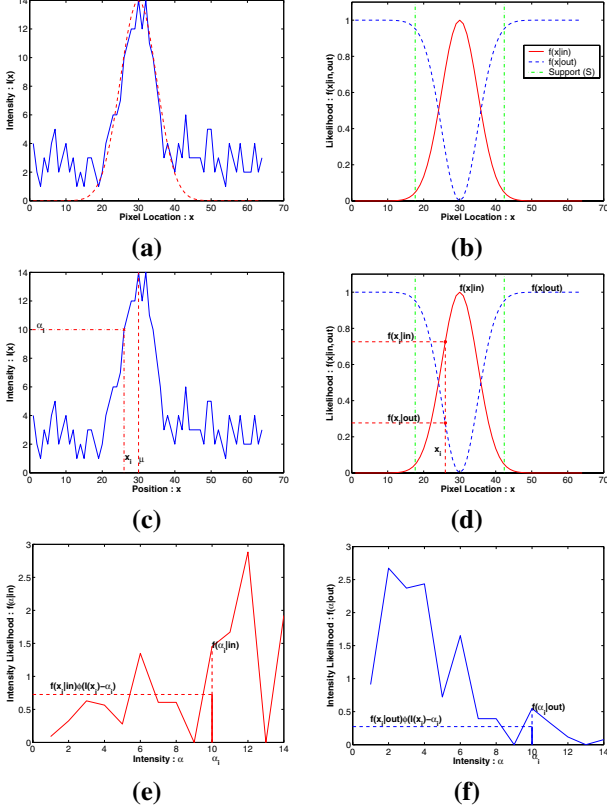


Figure 1: The likelihood estimation processes illustrated in a 1D toy example. (a) 1D noisy data with a Gaussian fitted by the pre-process (Sec. 2). (b) Foreground (solid) and background (dash) spatial likelihoods and the analysis support (dot-dash), derived from the Gaussian. (c) The toy data, showing a pair of pixel location and intensity value  $(\mathbf{x}_i, \alpha_i)$ . (d) The spatial likelihoods, showing the foreground and background likelihoods at  $\mathbf{x}_i$ . (e) Foreground intensity likelihood, showing contribution from the data point  $(\mathbf{x}_i, \alpha_i)$ . (f) Background intensity likelihood, showing contribution from  $(\mathbf{x}_i, \alpha_i)$ .

are normalized to 1 within this range  $S$ ,

$$\begin{aligned} \bar{P}(\mathbf{x}|in) &\equiv P(\mathbf{x}|in) / \int_S P(\mathbf{x}|in) d\mathbf{x} \\ \bar{P}(\mathbf{x}|out) &\equiv P(\mathbf{x}|out) / \int_S P(\mathbf{x}|out) d\mathbf{x} \end{aligned} \quad (6)$$

where  $P(\mathbf{x}|in)$  is assumed to be known (as given in Eq.(5)) and  $P(\mathbf{x}|out)$  is an unknown underlying background distribution function that is unnormalized over  $S$ . The total probability theorem states that,

$$P_{\mathbf{X}} = \bar{P}(\mathbf{x}|in)P_{in} + \bar{P}(\mathbf{x}|out)P_{out} \quad (7)$$

$$P_{in} + P_{out} = 1 \quad (8)$$

where  $P_{\mathbf{X}}$ ,  $P_{in}$ , and  $P_{out}$  are prior probabilities of the location  $\mathbf{x}$  and inside and outside labels in  $S$ .  $P_{\mathbf{X}}$  is supposed to

obey an independent uniform distribution. This yields,

$$\begin{aligned} P_{\mathbf{X}} &= \frac{1}{|S|} \\ |S| &= \int_S d\mathbf{x} \end{aligned} \quad (9)$$

Substituting Eq.(8) and Eq.(9) to Eq.(7) yields,

$$\bar{P}(\mathbf{x}|out) = \frac{(1/|S|) - \bar{P}(\mathbf{x}|in) * P_{in}}{(1 - P_{in})} \quad (10)$$

This is a general form of the background spatial probability distribution given the foreground model in  $S$ . It provides a family of probability distributions that are parameterized by the ratio of the prior probabilities and the support  $S$ . In the following, we evaluate a special case in which the priors for the inside and outside labels are equal so that  $P_{in} = P_{out} = 0.5$ . In this case, Eq.(10) reduces to,

$$\bar{P}(\mathbf{x}|out) = \frac{2}{|S|} - \bar{P}(\mathbf{x}|in) = \frac{2}{|S|} - \frac{P(\mathbf{x}|in)}{\int_S P(\mathbf{x}|in) d\mathbf{x}} \quad (11)$$

Suppose now that the background pdf over  $S$  assumes the value zero at the mean location  $\mathbf{u}$  where the Gaussian  $\Phi(\mathbf{x}; \mathbf{u}, \Sigma)$ , modeling the foreground pdf, takes its maximum:  $\bar{P}(\mathbf{u}|out) = 0$ . With this assumption, the normalization factor of  $\bar{P}(\mathbf{x}|in)$  can be written as a function of the support's volume  $|S|$ ,

$$\int_S P(\mathbf{x}|in) d\mathbf{x} = P(\mathbf{u}|in) \frac{|S|}{2} = \frac{|S|}{2|2\pi\Sigma|^{1/2}} \quad (12)$$

Note that this equation can be interpreted as a constraint for the unknown support  $S$  imposed by choosing a form of the background pdf with the above assumption. In Section 4.3, we will show that this constraint uniquely determines the support  $S$  with a specific parameterization. Therefore, the following derivations hold true only with a specific support that is a solution to Eq.(12).

Substituting Eq.(12) to Eq.(6) and Eq.(11) yields,

$$\begin{aligned} \bar{P}(\mathbf{x}|in) &= \frac{2}{|S|} |2\pi\Sigma|^{1/2} P(\mathbf{x}|in) \\ \bar{P}(\mathbf{x}|out) &= \frac{2}{|S|} (1 - |2\pi\Sigma|^{1/2} P(\mathbf{x}|in)) \end{aligned} \quad (13)$$

Finally, we define the foreground and background spatial likelihood functions as the conditional pdfs over  $S$  scaled by a fixed factor  $|S|/2$  so that they depend only on  $P(\mathbf{x}|in)$ ,

$$f(\mathbf{x}|in) \equiv \frac{|S|}{2} \bar{P}(\mathbf{x}|in) = |2\pi\Sigma|^{1/2} P(\mathbf{x}|in) \quad (14)$$

$$f(\mathbf{x}|out) \equiv \frac{|S|}{2} \bar{P}(\mathbf{x}|out) = 1 - |2\pi\Sigma|^{1/2} P(\mathbf{x}|in) \quad (15)$$

Note that the background likelihood  $f(\mathbf{x}|out)$  is a complement of the foreground likelihood. At the mean location  $\mathbf{u}$ , we have  $f(\mathbf{u}|in) = 1$  and  $f(\mathbf{u}|out) = 0$ . At the infinity,  $f(\pm\infty|in) = 0$  and  $f(\pm\infty|out) = 1$ . Fig.1(a,b) illustrate

the resulting spatial likelihood functions in a 1D toy example. Given the fitted Gaussian shown by a dash-curve in Fig.1(a), the foreground (solid) and background (dash) likelihoods are analytically determined as shown in Fig.1(b).

Because both fore- and back-ground likelihoods share the same scaling factor, the ratio of the likelihoods and that of the pdfs become equivalent. Furthermore, the conditional pdfs are also equivalent to the posterior distributions  $\bar{P}(in|\mathbf{x})$  and  $\bar{P}(out|\mathbf{x})$  since  $P_{in} = P_{out} = 0.5$ ,

$$\frac{f(\mathbf{x}|in)}{f(\mathbf{x}|out)} = \frac{\bar{P}(\mathbf{x}|in)}{\bar{P}(\mathbf{x}|out)} = \frac{\bar{P}(in|\mathbf{x})}{\bar{P}(out|\mathbf{x})} \quad (16)$$

## 4.2. Intensity Likelihood Functions

This section derives the intensity likelihood functions in the Bayesian framework. Modeling the foreground and background intensity likelihoods  $f(\alpha|in)$  and  $f(\alpha|out)$  given a VOI  $I(\mathbf{x} \in \Omega)$  is a chicken-and-egg problem; a segmentation result is required to estimate the fore- and back-ground likelihoods that are necessary for the segmentation itself. Instead of using the classical iterative approach, such as EM algorithm, our solution is based on weighted likelihood model approach avoiding the iterations. This approach exploits the spatial likelihoods, derived as functions of the fitted Gaussian function, as weights for modeling the intensity likelihoods without an explicit segmentation.

First we define the conditional intensity probability distributions as a function of intensity differences weighted by the corresponding spatial probability distributions in Eq.(6) and sampled within the analysis support  $S \subset \Omega$ ,

$$\begin{aligned} \bar{P}(\alpha|in) &\equiv \int_S \bar{P}(\mathbf{x}, \alpha|in) d\mathbf{x} \\ &= \int_S \bar{P}(\mathbf{x}|in) \phi(I(\mathbf{x}) - \alpha) d\mathbf{x} \\ \bar{P}(\alpha|out) &\equiv \int_S \bar{P}(\mathbf{x}, \alpha|out) d\mathbf{x} \\ &= \int_S \bar{P}(\mathbf{x}|out) \phi(I(\mathbf{x}) - \alpha) d\mathbf{x} \end{aligned} \quad (17)$$

where  $\bar{P}(\alpha|\mathbf{x}, \{in/out\})$  is modeled by  $\phi(I(\mathbf{x}) - \alpha)$ . In order to assure the unit-normalization over the support  $S$ , the function  $\phi$  can be set to the discrete Dirac delta function so as to construct a weighted histogram. For estimating a continuous pdf from a small number of samples, Parzen window with a uniform step kernel can be used as  $\phi$  while maintaining the unit-normalization. Substituting Eq.(13) to Eq.(17) yields,

$$\begin{aligned} \bar{P}(\alpha|in) &= \frac{2}{|S|} \int_S f(\mathbf{x}|in) \phi(I(\mathbf{x}) - \alpha) d\mathbf{x} \\ \bar{P}(\alpha|out) &= \frac{2}{|S|} \int_S f(\mathbf{x}|out) \phi(I(\mathbf{x}) - \alpha) d\mathbf{x} \end{aligned} \quad (18)$$

We define the intensity likelihood functions as scaled conditional pdfs with a fixed factor  $|S|/2$  sampled over the support  $S$ ,

$$f(\alpha|in) \equiv \frac{|S|}{2} \bar{P}(\alpha|in) = \int_S f(\mathbf{x}|in) \phi(I(\mathbf{x}) - \alpha) d\mathbf{x} \quad (19)$$

$$f(\alpha|out) \equiv \frac{|S|}{2} \bar{P}(\alpha|out) = \int_S f(\mathbf{x}|out) \phi(I(\mathbf{x}) - \alpha) d\mathbf{x} \quad (20)$$

Similar to the spatial likelihood case, the likelihood functions, the conditional pdfs and the posterior pdfs for foreground and background share the same scaling factor. Moreover, the intensity pdfs are also proportional to expected values of the counts of data with a specific intensity and a label. Therefore all these ratios become equivalent,

$$\frac{f(\alpha|in)}{f(\alpha|out)} = \frac{\bar{P}(\alpha|in)}{\bar{P}(\alpha|out)} = \frac{\bar{P}(in|\alpha)}{\bar{P}(out|\alpha)} = \frac{E[n_{\alpha,in}]}{E[n_{\alpha,out}]} \quad (21)$$

where  $E[n_{\alpha,\{in,out\}}]$  denotes the expectation of the number of data with the intensity  $\alpha$  and inside or outside of the target tumor.

The standard iterative approach for likelihood estimation requires pre-assigned foreground and background labels to each voxel during each iteration step. Our solution utilizes the spatial likelihood functions in the place of the pre-assigned labels, treating them as *soft* probabilistic segmentation. Since the first fitting step in Section 2 already provides robust and accurate target characterization, captured in  $f(\mathbf{x}|in)$  and  $f(\mathbf{x}|out)$ , the iterative model updates are not necessary for our solution.

Fig.1(c-f) illustrate the intensity likelihood estimation processes. Using all data within the support ( $\mathbf{x}_i \in S, \alpha_i$ ), the foreground (Fig.1(e)) and background (Fig.1(f)) intensity likelihoods are estimated by accumulating  $\phi$ -smoothed counts for each intensity value  $\alpha_i$  weighted by the corresponding spatial likelihoods  $f(\mathbf{x}_i|in)$  and  $f(\mathbf{x}_i|out)$  shown in Fig.1(d).

## 4.3. Analysis Support

The choice of the analysis support  $S$  is critical for the proposed segmentation solution. The spatial extent of background covers an infinite range of the data space  $\mathbf{x}$ . Thus a background spatial likelihood function is not bounded and cannot be normalized in the complete data space since the normalization factor becomes infinity. For this reason, the analysis support was introduced in Section 4.1 so that probability distributions can be defined within such a support. However, the estimated background likelihood will be sensitive to the varying range of  $S$  since such variation of the support  $S$  would cause a large change to the normalization factor. Determination of appropriate data space support is therefore a general problem for modeling background probability distribution.

We suggest that the support  $S$  should be considered as a function of the target scale. If a cup on a table is to be segmented, for example, it is sensible to model the background using specific information of the table, not of the house where the table is in nor of the city the house is in. In our case, the Gaussian function fitted to the target structure by the pre-process can provide such scale information in the form of a confidence ellipsoid of  $N$ -D equal-probability contour approximating the structure boundary. Utilizing this, we parameterize the analysis support  $S$  as a function of the ellipsoid,

$$S(c) \equiv \{\mathbf{x} | (\mathbf{x} - \mathbf{u})^t \boldsymbol{\Sigma}^{-1} (\mathbf{x} - \mathbf{u}) \leq c\} \quad (22)$$

where the scalar  $c$ , the Mahalanobis distance of  $\mathbf{x}$  from  $\mathbf{u}$  with covariance  $\boldsymbol{\Sigma}$ , uniquely determines  $S$ . The remaining task is to set the parameter  $c$  so that  $S$  covers all the extent of the target (e.g., cup) and a reasonable amount of the background (e.g., table).

In Section 4.1, we formally derived the spatial likelihood models in the Bayesian framework by assuming that the prior of label distributions within  $S$  is unbiased ( $P_{in} = P_{out}$ ) and that the normalized background spatial likelihood  $\bar{P}(\mathbf{x}|out)$  assumes 0 at the mean  $\mathbf{u}$  ( $\bar{P}(\mathbf{u}|out)=0$ ). These two assumptions in fact uniquely determine  $S(c)$ . In other words, employing the form of the spatial likelihoods in Eq.(5), Eq.(14) and Eq.(15) implicitly determines a specific  $S(c)$ . An integral equation of unknown  $S(c)$  satisfying these conditions can be derived from Eq.(12), which depends only on  $P(\mathbf{x}|in)$ ,

$$\begin{aligned} \int_S P(\mathbf{x}|in) d\mathbf{x} &= \frac{|S|}{2|2\pi\boldsymbol{\Sigma}|^{1/2}} \\ \Leftrightarrow |S(c)| &= \int_{S(c)} d\mathbf{x} \\ &= 2 \int_{S(c)} \exp(-1/2(\mathbf{x} - \mathbf{u})^t \boldsymbol{\Sigma}^{-1} (\mathbf{x} - \mathbf{u})) d\mathbf{x} \end{aligned} \quad (23)$$

The solution  $S(c)$  depends on the dimensionality  $N$  of the data space  $\mathbf{x}$ . For example, numerical solutions of Eq.(23) for 1D, 2D and 3D cases are:  $c_1 \approx 6.1152$ ,  $c_2 \approx 3.1871$ ,  $c_3 \approx 2.4931$ , respectively. Within this support, the probability mass of  $f(\mathbf{x}|in)$  and  $f(\mathbf{x}|out)$  over  $S$  are equivalent.

For the 3D segmentation,  $c_3 = 2.4931$  amounts to roughly 52% confidence interval of the chi-square distribution with three degrees of freedom. Empirically, our previous studies for 3D tumor segmentation showed that the equal-probability contour with  $c_3 = 1.6416$ , derived from 35% confidence interval of the fitted Gaussian function, approximates the tumor boundary well. This suggests that  $S(c_3)$ , resulted from our formal derivation, provides the data range that includes only a thin layer of background region around the target, covering the complete foreground and the background that only surrounds the target. This is an appropriate analysis support for modeling the background because the background model estimated over this support will not be strongly influenced by the non-target neighboring structures that may appear within  $\Omega$ .

#### 4.4. Joint Likelihood Ratio

The joint likelihood ratio  $r(\mathbf{x})$  defined in Eq.(3) can be expressed as a function of the fitted Gaussian  $\Phi(\mathbf{x}; \mathbf{u}, \boldsymbol{\Sigma})$  and the input data  $I(\mathbf{x})$  by using the form of spatial and intensity likelihood models derived in Sections 4.1 and 4.2,

$$r(\mathbf{x}) = \frac{|2\pi\boldsymbol{\Sigma}|^{1/2} \Phi(\mathbf{x}; \mathbf{u}, \boldsymbol{\Sigma}) \int_S |2\pi\boldsymbol{\Sigma}|^{1/2} \Phi(\mathbf{x}; \mathbf{u}, \boldsymbol{\Sigma}) \phi(I(\mathbf{x}) - \alpha) d\mathbf{x}}{(1 - |2\pi\boldsymbol{\Sigma}|^{1/2} \Phi(\mathbf{x}; \mathbf{u}, \boldsymbol{\Sigma})) \int_S (1 - |2\pi\boldsymbol{\Sigma}|^{1/2} \Phi(\mathbf{x}; \mathbf{u}, \boldsymbol{\Sigma})) \phi(I(\mathbf{x}) - \alpha) d\mathbf{x}} \quad (24)$$

This shows that the likelihood ratio at  $\mathbf{x}$  with intensity value  $\alpha$  depends only on  $\Phi(\mathbf{x}; \mathbf{u}, \boldsymbol{\Sigma})$  and  $I(\mathbf{x} \in S)$ .

The formal derivations presented in Sections 4.1 and 4.2 also assure that the ratios of the foreground and background likelihoods are equivalent to the ratios of the posterior pdfs normalized over the analysis support  $S(c)$ . Thus we can rewrite  $r(\mathbf{x})$  with such posterior pdfs given the independence of  $\mathbf{x}$  and  $\alpha$  and  $P_{in} = P_{out}$ ,

$$r(\mathbf{x}) = \frac{\bar{P}(in|\mathbf{x}) \bar{P}(in|\alpha)}{\bar{P}(out|\mathbf{x}) \bar{P}(out|\alpha)} = \frac{\bar{P}(in|(\mathbf{x}, \alpha))}{\bar{P}(out|(\mathbf{x}, \alpha))} \quad (25)$$

This justifies the joint likelihood ratio test segmentation in Eq.(4) as the optimal Bayesian binary classification of each voxel when the likelihoods defined in this section are used and the LRT threshold  $th$  in Eq.(4) is set to one.

### 5. Algorithm Overview

The following summarizes the proposed semi-automatic  $N$ -D figure-ground segmentation algorithm.

#### STEP1: Robust Anisotropic Gaussian Fitting [12, 14]:

Given a volumetric data  $I(\mathbf{x})$  and a marker  $\mathbf{x}_p$  indicating rough location of the target blob structure,

1. Extract a volume of interest (VOI= $I(\mathbf{x} \in \Omega)$ ) centered at  $\mathbf{x}_p$ .
2. Perform the anisotropic Gaussian fitting, resulting in the robust estimate of target center  $\mathbf{u}$  and anisotropic spread  $\boldsymbol{\Sigma}$ .

#### STEP2: Joint Likelihood Ratio Test Segmentation:

Given the estimated target center and spread ( $\mathbf{u}, \boldsymbol{\Sigma}$ ) and the VOI  $I(\mathbf{x} \in \Omega)$ ,

1. Estimate the foreground and background intensity likelihoods  $f(\alpha|in)$  and  $f(\alpha|out)$  over the analysis support  $S(c_N)$  using Eq.(14), Eq.(15), Eq.(19), Eq.(20), and Eq.(22).
2. For each voxel ( $\mathbf{x} \in S(c_N), \alpha$ ),
  - (a) Compute the likelihood ratio  $r(\mathbf{x})$  in Eq.(3) using Eq.(14) and Eq.(15) and pre-computed  $f(\alpha|in)$  and  $f(\alpha|out)$ .
  - (b) Perform the likelihood ratio test in Eq.(4) and assign the *label*  $\in \{in, out\}$  to  $(\mathbf{x}, \alpha)$ .

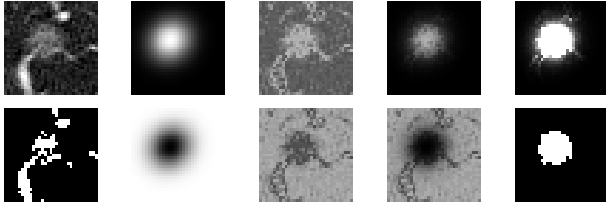


Figure 2: 2D cross sections of 3D likelihood functions, likelihood ratio, and segmentation results estimated for a non-solid GGO nodule with a vessel. Top row (left to right): input  $I(\mathbf{x})$ , foreground spatial likelihood  $f(\mathbf{x}|in)$ , foreground intensity likelihood  $f(\alpha|in)$ , joint foreground likelihood  $f(\mathbf{x}, \alpha|in)$ , joint likelihood ratio  $r(\mathbf{x})$ . Bottom row: FWHM segmentation result, background intensity likelihood  $f(\alpha|out)$ , joint background likelihood  $f(\mathbf{x}, \alpha|out)$ , segmentation result by the proposed method.

## 6. Experimental Results

A 3D implementation of the proposed method is applied to volumetric lung tumor segmentation problem: delineating a target lung nodule from background lung parenchyma with the presence of other non-target structures such as vessels and lung walls. Its performance is evaluated by using high resolution chest CT images of 39 patients including 1310 lung nodules. The images are of size  $512 \times 512 \times 400$  voxels (depth slightly varies across the patients) with 12 bit intensity range. For each lung tumor, a rough location marker is provided by an expert radiologist. The size of VOI is fixed to  $33 \times 33 \times 33$  voxels. The width of the uniform kernel  $\phi$  is set to 512. The same parameter settings from [14] are used for the robust Gaussian model fitting part.

Fig.2 shows 2D cross sections of various 3D likelihood functions and resulting segmentations estimated for a non-solid ground-glass opacity (GGO) nodules with an attached vessel (top-left). The non-solid GGO nodules appear in CT scans as small noisy (non-Gaussian) intensity distributions with relatively low intensity values. A recent clinical study reported that this type of nodules have high likelihood for developing into malignant tumors [5]. However, no generic and effective solution to segment this type of tumors has been proposed. It is difficult to segment such tumors effectively by threshold-based methods such as [8]. The bottom-left image in Fig.2 displays a segmentation result by the conventional full-width-at-half-maximum (FWHM) scheme, illustrating such a case. Our method provides correct segmentation (bottom-right) even with the presence of the vessel acting as a non-target neighboring structure.

Fig. 3 shows examples of 2D views of 3D segmentation results for five tumor cases. Results for both the anisotropic Gaussian fitting and the joint LRT segmentation are shown in the middle and right column of the figure, respectively.

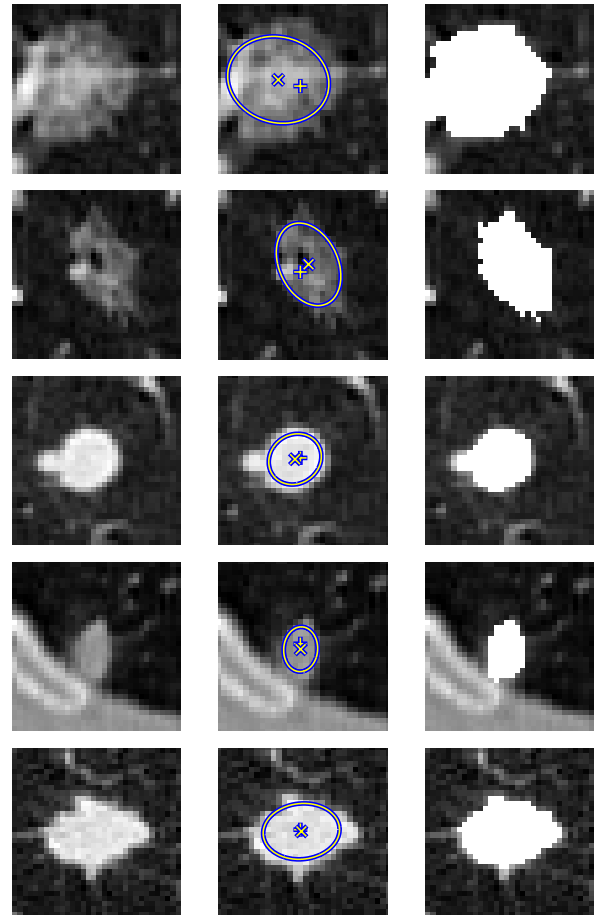


Figure 3: Five examples of segmentation results shown in 2D cross section passing through the estimated tumor center  $\mathbf{u}$ . Left column: input data. Middle column: anisotropic Gaussian fitted to the data by the method in Sec 2; "+" marker  $\mathbf{x}_p$ , "x": estimated center  $\mathbf{u}$ , ellipses: image-plane intersection of 35% confidence ellipsoid of the estimated Gaussian. Right column: segmentation results shown as grayscale images with the segmented regions filled in with white (255) value.

They illustrate the proposed method's capability to handle irregular 3D boundary geometries. The fourth row of the figure also illustrates that the case with the presence of neighboring lung wall was segmented correctly.

With the total of 1310 tumor cases, the Gaussian fitting pre-process successfully approximated the tumor boundary for 1139 cases. Our solution and the 4D space-intensity joint-domain mean shift solution [13, 2] are compared using these 1139 cases. The error rates, confirmed manually by expert's eye-appraisal, were 5% (52 cases) for our solution and 7% (77 cases) for the mean shift solution. The most of failures by our solution were due to a few isolated voxels near the target boundary being falsely segmented as

a part of the target when non-target structures were present nearby. This can be mitigated by performing a connected component analysis as a post-process. After such a post-process, the error rate reduces to only 1% (11 cases). Also, our solution significantly improves run-time efficiency. In average, our solution runs in less than 3 seconds with a 2.4 GHz Pentium IV processor that is 3 times faster than the mean shift solution.

## 7. Conclusion

This paper presented a robust, efficient, and accurate, semi-automatic framework for segmenting the blob-like structures in multi-dimensional images. The solution is realized by combining the robust anisotropic Gaussian model fitting and the likelihood ratio test (LRT)-based non-parametric segmentation in the joint space-intensity domain. The unification is achieved by exploiting the fitted anisotropic Gaussian as a spatial prior for modeling the likelihood functions used in the latter non-parametric segmentation. We also demonstrated that the LRT with its threshold set to one becomes equivalent to the optimal Bayesian binary classification, when the likelihoods are estimated over the formally derived analysis support. One of the advantages of our solution is that the likelihood functions are estimated for each data instance so that it provides robust segmentation results regardless of different data acquisition settings without tuning threshold parameters.

A 3D implementation of the proposed method is also successfully applied to the problem of volumetric lung tumor segmentation. Our experimental results demonstrated that the proposed solution successfully and efficiently delineates the irregular tumor boundary even for the difficult non-solid GGO cases. Such technology can enhance the accuracy and usability of the current state-of-the-art volumetric tumor quantification and visualization methods for computer-aided diagnosis applications, assisting to improve overall medical diagnostic efficacy.

There are a number of open issues we plan to address in near future. The final segmentation results of our solution depends on the correct model fitting by the first part. In order to further improve the overall performance, therefore, we plan to improve the performance of the anisotropic Gaussian model fitting by revising its automatic bandwidth selection process. Furthermore, the proposed LRT-based segmentation framework is not fundamentally restricted to the Gaussian spatial prior used in this study. The extension of our modeling solutions towards other types of functional forms also remains as our future work.

## Acknowledgments

We thank Maneesh Singh, Claus Bahlmann, Dorin Comaniciu, Visvanathan Ramesh for stimulating discussions and comments, and Jonathan Stoeckel for his supports.

## References

- [1] Y. Boykov, O. Veksler, and R. Zabih. Fast approximate energy minimization via graph cuts. *PAMI*, 20:1222–39, 2001.
- [2] D. Comaniciu and P. Meer. Mean shift: A robust approach toward feature space analysis. *PAMI*, 24:603–619, 2002.
- [3] W. Feller. *An Introduction to Probability Theory and Its Applications*, volume 2. Wiley, New York, 1971.
- [4] S. Geman and D. Geman. Stochastic relaxation, Gibbs distributions, and the Bayesian restoration of images. *PAMI*, 6:721–741, 1984.
- [5] C. I. Henschke et al. CT screening for lung cancer: frequency and significance of part-solid and non-solid nodules. *Am. J. Roentgenol.*, 178:1053–1057, 2002.
- [6] M. Kass, A. Witkin, and D. Terzopoulos. Snakes: Active contour models. *IJCV*, 1:321–331, 1987.
- [7] J. J. Koenderink. The structure of images. *Biol. Cybern.*, 50:363–370, 1984.
- [8] W. J. Kostis et al. Three-dimensional segmentation and growth-rate estimation of small pulmonary nodules in helical CT images. *IEEE TMI*, 22:1259–1274, 2003.
- [9] A. Leonardis, A. Gupta, and R. Bajcsy. Segmentation of range images as the search for geometric parametric models. *IJCV*, 14:253–277, 1995.
- [10] M. Loog, J. J. Duistermaat, and L. M. J. Florack. On the behavior of spatial critical points under Gaussian blurring. In *Scale-Space*, pages 183–192, 2001.
- [11] M. Meila and J. Shi. Learning segmentation by random walks. In *NIPS*, 2001.
- [12] K. Okada, D. Comaniciu, N. Dalal, and A. Krishnan. A robust algorithm for characterizing anisotropic local structures. In *ECCV*, pages 1:549–561, 2004.
- [13] K. Okada, D. Comaniciu, and A. Krishnan. Robust 3D segmentation of pulmonary nodules in multislice CT images. In *MICCAI*, pages II:881–889, 2004.
- [14] K. Okada, D. Comaniciu, and A. Krishnan. Scale selection for anisotropic scale-space: Application to volumetric tumor characterization. In *CVPR*, pages I:594–601, 2004.
- [15] S. Osher and N. Paragios. *Geometric Level Set Methods in Imaging, Vision, and Graphics*. Springer, New York, 2003.
- [16] J. V. Pastor, J. Arregle, and A. Palomares. Diesel spray image segmentation with a likelihood ratio test. *Applied Optics*, 40:2876–2885, 2001.
- [17] A. P. Reeves and W. J. Kostis. Computer-aided diagnosis of small pulmonary nodules. *Seminars in Ultrasound, CT, and MRI*, 21:116–128, 2000.
- [18] J. Shi and J. Malik. Normalized cuts and image segmentation. *PAMI*, 22:657–673, 2000.
- [19] A. Witkin. Scale-space filtering. In *IJCAI*, pages 1019–1021, Karlsruhe, 1983.
- [20] S. C. Zhu and A. Yuille. Region competition: Unifying snakes, region growing, and Bayes/MDL for multiband image segmentation. *PAMI*, 18:884–900, 1996.